# The tomato *fer* gene encoding a bHLH protein controls iron-uptake responses in roots

**Hong-Qing Ling*[†‡], Petra Bauer[†§¶], Zsolt Bereczky[§], Beat Keller*, and Martin Ganal[§‖]**

[§]Institute of Plant Genetics and Crop Plant Research, Correnstrasse 3, D-06466 Gatersleben, Germany; and *Institute of Plant Biology, University of Zürich, Zollikerstrasse 107 CH-8008 Zürich, Switzerland

Edited by John H. Law, University of Arizona, Tucson, AZ, and approved September 3, 2002 (received for review July 29, 2002)

**Iron deficiency is among the most common nutritional disorders in plants. To cope with low iron supply, plants with the exception of the Gramineae increase the solubility and uptake of iron by inducing physiological and developmental alterations including iron reduction, soil acidification, Fe(II) transport and root-hair proliferation (strategy I). The chlorotic tomato *fer* mutant fails to activate the strategy I. It was shown previously that the *fer* gene is required in the root. Here, we show that *fer* plants exhibit root developmental phenotypes after low and sufficient iron nutrition indicating that FER acts irrespective of iron supply. Mutant *fer* roots displayed lower *Leirt1* expression than wild-type roots. We isolated the *fer* gene by map-based cloning and demonstrate that it encodes a protein containing a basic helix–loop–helix domain. *fer* is expressed in a cell-specific pattern at the root tip independently from iron supply. Our results suggest that FER may control root physiology and development at a transcriptional level in response to iron supply and thus may be the first identified regulator for iron nutrition in plants.**

Plants are the most valuable source of nutrients for the human world population. The production of nutrient-rich crops is therefore a major aim of biotechnology (1). Iron deficiency is the most common human nutritional disorder in the world (1, 2). Iron is an essential cofactor for two important biological processes, photosynthesis and nitrogen fixation, and the availability of iron greatly influences plant growth (3–5). Although iron is abundant in soil, it is present almost exclusively in its oxidized, low-soluble form Fe(III), which is often not readily available to plants, especially in alkaline soils (5). Sessile plants need to adapt their root physiology and morphology to acquire iron from their environment efficiently. After iron starvation, dicot and monocot (except grass) roots display a series of morphological and physiological reactions known as strategy I to increase iron solubility and uptake (6). Strategy I includes the induction of iron-reductase activity at the root surface of the root-hair zone, proton extrusion, the activation of a high-affinity transport system for the uptake of Fe(II) in the root epidermis, and root-hair proliferation at the root tip (7–9). Strategy I responses are tightly regulated in response to iron availability. Expression of the iron-reductase genes *Atfro2* and *Psfro1* are induced by iron starvation in *Arabidopsis* and pea (10, 11). The Fe(II) transporter gene *Atirt1* in *Arabidopsis* is induced rapidly or switched off after changes of iron availability (9, 12, 13). In tomato, *Leirt1* expression is increased in low iron- versus sufficient iron-supply conditions (14). Moreover, ATIRT1 is subject to posttranslational protein-stability regulation (13). After sufficient iron supply, ATIRT1 may become ubiquitinated and degraded (13). The plant tissues involved in sensing the iron status and the nature of regulator proteins and signal molecules that communicate the iron-supply changes to the level of DNA are unknown. It can be expected that the manipulation of regulatory components will have profound influences on iron uptake. The most promising clues on the regulation of strategy I are expected from the identification of the *fer* gene. The *fer* (T3238*fer*) mutant is not able to switch on strategy I responses after iron deficiency, such as enhanced extrusion of protons and Fe(III)-chelate reductase activity in the root (15, 16). Reciprocal grafting of the mutant to a wild type indicated that the *fer* gene is required in roots but not in shoots (15). Genetic analysis showed that the *fer* mutation is a monogenic, recessive trait located on chromosome 6 of tomato (17). Here, we describe the isolation and characterization of the *fer* gene.

## Materials and Methods

**Plant Growth.** Tomato (*Lycopersicon esculentum*) seedlings were grown in a hydroponic system in Hoagland solution (18). Twelve days after germination, the plants were supplied with either 0.1 $\mu$M (iron limitation) or 10 $\mu$M (sufficient iron supply) FeNaEDTA in the Hoagland solution for up to 8 days. Then, plants were analyzed for iron-reductase activity (18). A morphological analysis was performed by using the lines T3238*fer* and T3238*FER*.

**Gene Isolation and Sequence Analysis.** Mapping and yeast artificial chromosome (YAC)-screening procedures were performed according to refs. 17 and 19. Bacterial artificial chromosome (BAC) clones were obtained from Molecular Genetics and analyzed and sequenced by using the shotgun-sequencing method as described (20, 21). ORFs were detected by using the MAPDRAW 4.0 program (DNAstar, Madison, WI) and by BLAST searches in databases. A full-length cDNA clone for ORFb (*fer*) was isolated from a root cDNA library of iron deficiency-induced *L. esculentum* cv. *Moneymaker* roots (SMART cDNA library-construction kit, CLONTECH).

**Complementation of the *fer* Mutant.** ORFb cDNA fragments of two different sizes (C1-2 and C2-8, respectively) were amplified from cDNA (forward primers 5′-aggatctagaatggagagtggtaatgcatcaatgga-3′ and 5′-aggatctagaatggaaaataataatgttaatgatattgggc-3′ for C1-2 and C2-8 constructs, respectively, and reverse primer 5′-aggatctagattagaccaacggagatgtctcgaag-3′ for both constructs) and cloned into pBINAR in sense orientation behind the 35S promoter (22). Whereas the coding sequence of the *fer* clone C1-2 started with the first identified ATG, the coding sequence of the *fer* clone C2-8 began with the second ATG, thus being 21 bp shorter than C1-2. ORFa was cloned as a 5,730-bp genomic *Eco*RV fragment into pBINAR. Transgenic *fer* (T3238*fer*) plants containing the C1-2, C2-8, and ORFa constructs were generated as described by using *Agrobacterium*

This paper was submitted directly (Track II) to the PNAS office.

Abbreviations: YAC, yeast artificial chromosome; BAC, bacterial artificial chromosome; RFLP, restriction fragment-length polymorphism; bHLH, basic helix–loop–helix.

Data deposition: The sequence reported in this paper has been deposited in the GenBank database (accession no. AF437878).

[†]H.-Q.L. and P.B. contributed equally to this work.

[‡]Present address: State Key Laboratory of Plant Cell and Chromosome Engineering, Institute of Genetics and Developmental Biology, Chinese Academy of Sciences, Datun Road, Andingmenwai, Beijing 100101, People's Republic of China.

[¶]To whom correspondence should be addressed. E-mail: bauer@ipk-gatersleben.de.

[‖]Present address: TraitGenetics GmbH, Am Schwabeplan 1b, D-06466 Gatersleben, Germany.

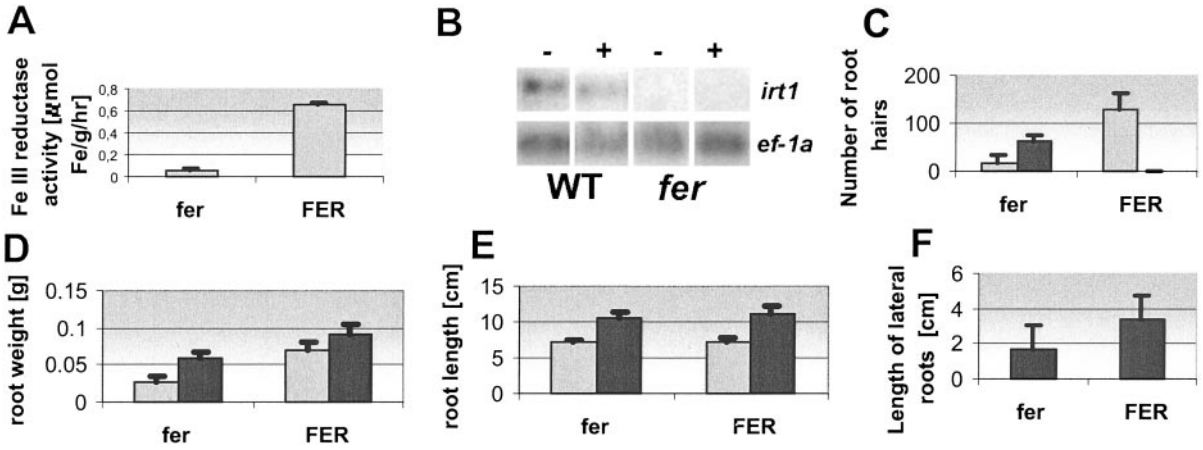


**Fig. 1.** Phenotypes of *fer* mutant and wild-type plants. (*A*) Iron reductase activity after iron limitation per gram of root per plant, $n = 7$–15 plants (see also ref. 15). (*B*) RT-PCR analysis of *Leirt1* expression in iron-deficient (−) and iron-sufficient (+) roots. (*C*) Number of root hairs within 2-mm segments of lateral root tips, $n = 25$ root tips. (*D*) Root weight per plant, $n = 7$–15 plants. (*E*) Length of the root system per plant, $n = 7$–15 plants. (*F*) Length of lateral roots initiated within the 3-cm segments of the main roots containing the main root tip, $n = 25$–30 lateral roots. Light gray columns, 0.1 $\mu$M iron; black columns, 10 $\mu$M iron.

*tumefaciens* (23). Transformation and regeneration was feasible *in vitro*, because *fer* plants were able to grow on Murashige–Skoog medium. Kanamycin-resistant regenerated plants were transferred into soil in the greenhouse for phenotypic observation and further analysis. Seven ORFa, four C1-2, and six C2-8 regenerated plants contained a transgene as verified by Southern blot analysis. ORFa transformants died soon after their transfer into soil. However, ORFb C1-2 and C2-8 lines grew to maturity, and seeds were harvested. A detailed analysis was performed on the progenies of single-insertion C1-2 and C2-8 lines.

**Gene-Expression Analysis.** Gene expression was analyzed in *L. esculentum* cv. *Moneymaker* plants. mRNA expression was analyzed by RT-PCR followed by agarose-gel electrophoresis and Southern blot hybridization (24). Intron-flanking oligonucleotides were used to amplify *fer* (5′-ttgcaacaaagggcgacacatt-3′ and 5′-ttacaataataacatgatattagaccaacgga-3′, 25 cycles), *Leef-1a* (5′-actggtggttttgaagctggtatctcc-3′ and 5′-cctcttgggctcgttaatctggtc-3′, 15 cycles) (25), and *Leirt1* sequences (5′-gcactttgctttcatcaaatgtttg-3′ and 5′-ttgcaactcccaataggtcatgaag-3′, 20 cycles) (14). For *in situ* hybridization analysis, root tips of 3-week-old plants were harvested after 9 days of growth in hydroponic Hoagland solution containing 0.1 or 10 $\mu$M FeNaEDTA, fixed, and embedded in paraplast (26). *In situ* hybridization was performed on 10-$\mu$m transverse root sections by using digoxigenin-labeled RNA probes (27). The *fer* antisense probe was derived from a subcloned cDNA fragment generated with the oligonucleotides 5′-atggagagtggtaatgcatcaatgga-3′ and 5′-tgattgctggataataggttgtgaaaat-3′. Positive hybridization signals were observed as violet staining due to the alkaline phosphatase reaction. In control *in situ* hybridization experiments labeled sense, *fer* transcripts were used as probe.

## Results

**The *fer* Mutant Is Affected in Molecular, Developmental, and Physiological Responses to Iron.** Under low-iron growth conditions (0.1 $\mu$M iron), *fer* mutant plants were highly chlorotic and died after two to three small leaves had emerged. In contrast, wild-type plants were hardly chlorotic and survived (not shown). *fer* mutant roots did not show the typical iron-reductase activity as observed in wild-type roots (ref. 15; Fig. 1*A*). Expression of the iron transporter gene *Leirt1* was at a low level compared with wild-type plants (Fig. 1*B*). Whereas wild-type lateral root tips had proliferating root hairs, *fer* root tips remained with few root hairs close to the tip (Fig. 1*C*). The root weight was significantly higher in wild-type roots than in *fer* roots (Fig. 1*D*). Presumably the reduced root weight in *fer* plants was due to decreased elongation of lateral roots. However, with the large variation in lateral root length, it was difficult to obtain significant numbers at the low iron-supply condition. Root growth at low iron supply generally was not inhibited in *fer*, because the root systems of *fer* mutant plants were of similar lengths as those of wild-type plants (Fig. 1*E*). Sufficient iron supply (10 $\mu$M iron) had a stimulating effect on root growth in both *fer* and wild-type plants (Fig. 1 *D* and *E*). *fer* mutant plants at sufficient iron concentrations displayed chlorotic leaves, although to a lower extent than at low iron concentrations (not shown). Wild-type plants had significantly longer lateral roots, fewer root hairs close to the tip, and higher *Leirt1* expression than *fer* plants (Fig. 1 *B*, *C*, and *F*). Thus, the *fer* mutation affected not only the physiological but also the root morphological and molecular responses at low and sufficient iron supply.

**Isolation of the *fer* Gene.** The *fer* gene was mapped previously to a 2.3-centimorgan interval between restriction fragment-length polymorphism (RFLP) markers TG590 and TG118 on chromosome 6 of tomato by using a mapping population derived from the T3238*fer* × LA716 cross (*Lycopersicon pennellii*) (17). For map-based cloning, the mapping population was expanded to 1,815 phenotypically scored $F_2$ plants. A high-resolution genetic map of the *fer* region showed that the *fer* gene was flanked by RFLP marker TG590 at a distance of 0.33 centimorgans (6 recombinants) and at a distance of 1.8 centimorgans (34 recombinants) by TG118 (Fig. 2*A*). Chromosome walking toward the *fer* gene was initiated from TG590 by using a YAC and BAC library of tomato (Fig. 2; *Materials and Methods*). The BAC clone 56B23 (≈210 kb) encompassed the entire *fer* region. Mapping analysis showed that the left end of BAC 56B23 (56R) cosegregated with the YAC ends 328N1 and 267AR. The right end of BAC 56B23 (56F) could not be mapped because of the presence of repetitive DNA sequences. BAC clone 53M23 (≈130 kb) hybridized only to the 337xsD probe. The left end of BAC 53M23 (53R) cosegregated with the *fer* gene, whereas the right end (53F) was mapped to two recombination events from the *fer* gene between *fer* and TG118 (Fig. 2*A*). Fingerprinting analysis of the two BAC clones revealed that the BAC clone 53M23 was contained fully within clone 56B23 suggesting that the 210-kb-large BAC 56B23 indeed contained the *fer* gene.

BAC clone 56B23 was sequenced fully by the shotgun-

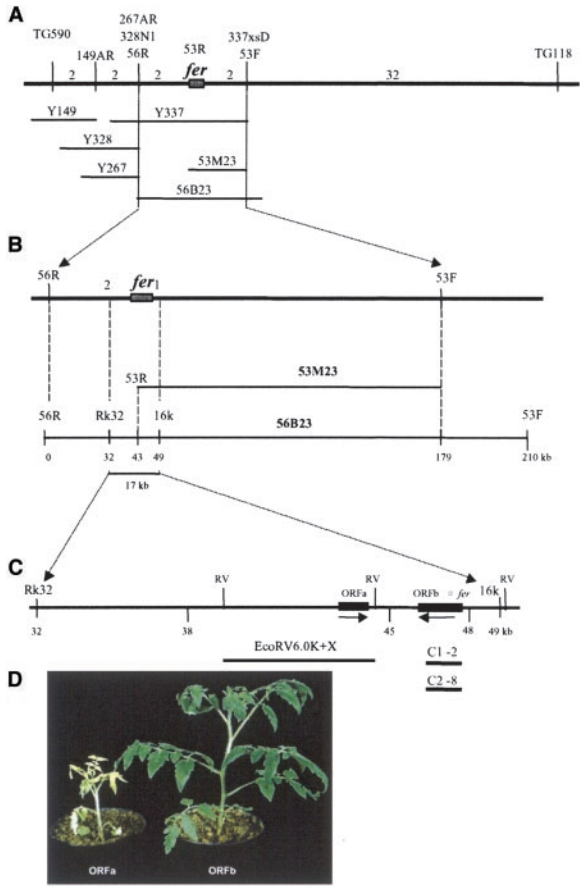


**Fig. 2.** Map-based cloning of the *fer* gene. (*A*) High-resolution genetic map of the *fer* region and establishment of a YAC and BAC contig. The *fer* gene (gray box) was located within the region ranging from RFLP markers TG590 to TG118 on chromosome 6 (bold line). The genetic locations of markers are indicated as vertical lines. Numbers above the bold line designate recombination events between the indicated markers. Horizontal lines below the *fer* region indicate the locations of YAC and BAC clones. (*B*) Genetic and physical location of markers derived from the sequence of BAC 56B23 and BAC 53M23. Rk32 and 16k are RFLP markers developed based on BAC-sequencing data. Numbers above the bold line designate recombination events between the indicated markers and *fer*. The numbers below the line representing BAC 56B23 indicate the physical distance of the respective markers in kilobases from the left end of the BAC clone. (*C*) Analysis of the 17-kb region containing the *fer* gene. ORFa and ORFb are two ORFs detected by the sequence analysis. Arrows indicate the direction of the ORF. RV represents *Eco*RV restriction sites. C1-2 and C2-8 represent two cDNA constructs of *fer* used for complementation. EcoRV6.0K+X is a genomic transformation construct containing ORFa. (*D*) Transgenic *fer* plants containing the ORFa construct (noncomplemented) and the ORFb C1-2 construct (complemented): C2-8 complemented similarly.

sequencing method (20, 21), and new RFLP markers were developed and mapped. In this way, the *fer* gene was delimited to a 17-kb region between Rk32 and 16k flanked by two and one recombination events, respectively (Fig. 2*B*). Two ORFs could be detected within the 17-kb DNA sequence, ORFa and ORFb (Fig. 2*C*). ORFa showed similarities with genes encoding transposases such as a Tam3-like transposon protein (GenBank accession no. AC035249). ORFb showed significant sequence similarity to genes harboring a conserved basic helix–loop–helix (bHLH) motif.

To prove the identity of the *fer* gene, transgenic plants homozygous for *fer* were generated harboring T-DNA (portion of the tumor-inducing plasmid that is transferred to plant cells) constructs with an intact ORFa and intact ORFb, respectively. After their transfer into soil, ORFa transformants had developed yellow and necrotic leaves and died soon after, whereas ORFb transformants remained green and healthy, indicating that only the latter ones were complemented (Fig. 2*D*). ORFb-transformed plants with both C1-2 and C2-8 constructs grew to maturity and set fruits. A detailed analysis was performed on the selfed progeny from transgenic ORFb plants harboring single C2-8 and C1-2 T-DNA insertions, respectively. The progeny segregated 1:3 into nontransgenic short and highly chlorotic plants devoid of reductase activity and transgenic taller chlorotic plants with reductase activity after low iron supply (Fig. 3 *A* and *B*). The shoot appearance was comparable between *fer* mutant and nontransgenic *fer* individuals as well as between wild-type and transgenic individuals. With respect to root weight and root-hair proliferation, transgenic *fer* plants appeared similar to wild-type plants in contrast to their nontransgenic siblings (Fig. 3 *C* and *D*). Root-hair proliferation, however, appeared less pronounced in the complemented transgenic plants compared with the TFER wild-type line. *Leirt1* expression was higher in the complemented transgenic plants than in the nontransgenic siblings (Fig. 3*E*). Taken together, the ORFb transgene cosegregated with the complementation of *fer* plants in the progeny tests. Thus, the mapping data and complementation tests demonstrated that ORFb indeed was the *fer* gene.

**Structural Analysis of the *fer* Gene Encoding a bHLH Protein.** Comparing the cDNA and genomic *fer* sequences, it was found that the *fer* gene contained four exons and three introns (Fig. 4*A*). Exons 1 and 2 contained a region coding for a highly conserved bHLH motif characteristic for the family of eukaryotic bHLH transcriptional regulatory proteins (ref. 28; Fig. 4 *A* and *B*). Outside of the conserved putative DNA-binding domain, similarity was found only to a predicted *Arabidopsis* protein of similar size (GenBank accession no. AF488570, 42.5% identity and 72% similarity), suggesting that *fer* might represent a conserved transcriptional regulator gene in dicotyledonous plants (not shown). A putative *fer* homolog from rice could not be identified by database comparisons.

By using the *fer* cDNA as probe, a restriction fragment-length DNA polymorphism was detected between T3238*fer* and its wild-type parent T3238*FER*, which indicated that the mutation of T3238*fer* was caused either by the insertion of a DNA fragment or a genomic rearrangement within the *fer* region (Fig. 4*C*). By using various primer combinations designed from the genomic *fer* DNA sequence, a region of 136 bp at the end of exon 1 could be delimited and could not be amplified by PCR from *fer* mutant plants (Fig. 4*D*). This observation indicated that most likely a large DNA insertion was present at the end of exon 1.

***fer* Is Expressed in Roots in a Cell-Specific Manner.** To investigate in which parts of the plants the *fer* gene is active, *fer* expression was analyzed in various tissues of tomato plants. Expression of *fer* was detected in roots and root tips and at a lower level in hypocotyls of seedlings (Fig. 5*A*). No transcripts were detected in cotyledon and leaf samples. *fer* expression remained at a comparable level in root samples taken from plants that were transferred into growth medium containing either 0.1 or 10 $\mu$M iron for 6 h up to 8 days (Fig. 5*B*). The expression levels were not altered significantly if plants were exposed to 50 $\mu$M iron (data not shown). These observations indicated that the expression of *fer* occurred in a root-specific manner independently from the iron concentration in the growth medium.

Localization of *fer* gene expression in root tips showed that in the dividing root zone following the root meristem where no differentiation of the vascular system had occurred yet, *fer* expression was detected in the root epidermis as well as the outer cortical cell layers (Fig. 6*D*). In the elongation and young

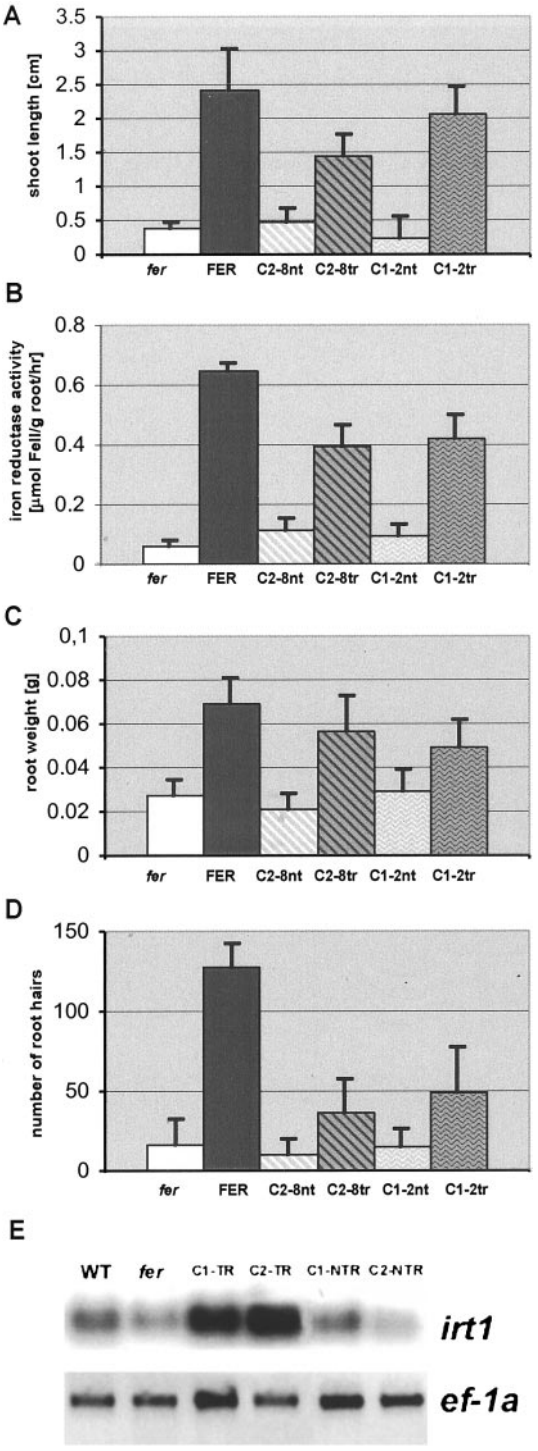


**Fig. 3.** Phenotypic analysis of segregating progenies of two complemented transgenic *fer* plants containing a single ORFb T-DNA insertion of C2-8 and C1-2, respectively. The genotypes of the progeny were confirmed by Southern blot hybridization and PCR. The experiments were performed on plants grown at 0.1 $\mu$M iron. *fer* and FER are the control lines T3238*fer* and T3238*FER*. C2-8nt and C1-2nt regroup the nontransgenic individuals. C2-8tr and C1-2tr regroup the transgenic individuals. (*A*) Average length of the shoots per plant measured between the hypocotyls and shoot apex. (*B*) Average root iron-reductase activity per gram root per plant. (*C*) Average weight of the root system per plant. (*D*) Average number of root hairs per 2-mm section containing a lateral root tip. (*E*) RT-PCR expression analysis of *Leirt1* in roots of wild type and *fer* as well as the transgenic (TR) and nontransgenic (NTR) C1-2 (C1) and C2-8 (C2) lines. As positive control, expression of elongation factor *Leef-1a* was monitored.

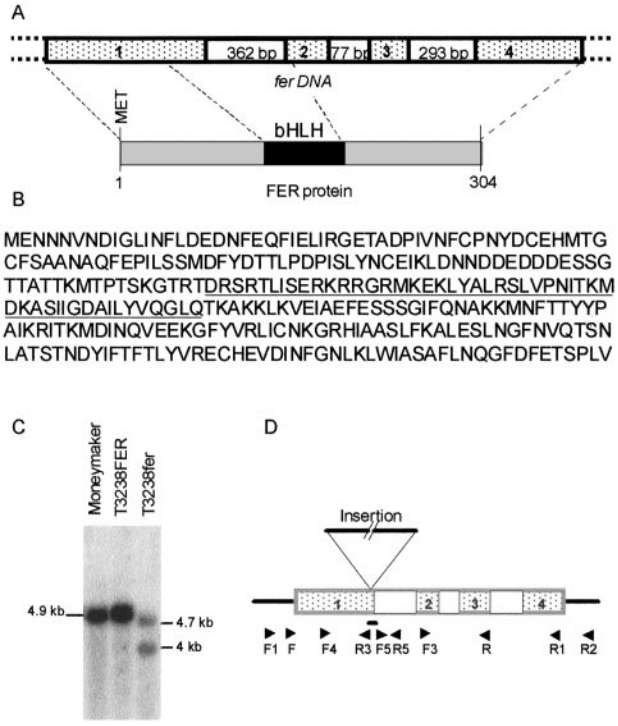


**Fig. 4.** Structural analysis of the *fer* gene. (*A*) Gene structure of *fer*. The upper drawing shows in hatched boxes exons 1–4 separated by three introns indicated by white boxes. The lengths of the three introns are indicated in base pairs. The lower part shows the structure of the predicted protein gene product. The black box delimits the position of the bHLH domain. (*B*) Predicted amino acid sequence encoded by the *fer* gene. The underlined amino acids form the bHLH motif. (*C*) RFLP of the *fer* alleles of the mutant T3238*fer* and the wild-type lines *L. esculentum* T3238*FER* (progenitor of T3238*fer*) and cv. *Moneymaker*. Genomic DNA was digested with *Eco*RV and probed with the *fer* cDNA. (*D*) Location of the insertion in the *fer* allele of T3238*fer*. Arrowheads indicate the positions of various primers used for amplification of different regions of the *fer* gene. The black bar between R3 and F5 indicates the DNA region that could not be amplified by PCR with any primer combination from the mutant, indicating that a large insertion was present in this region.

root-hair zone where the vascular cylinder started to differentiate, *fer* transcripts were found in the root epidermis mainly and occasionally at a low level in the cortical cells (Fig. 6*C*). In the mature root-hair zone, *fer* expression was found to be restricted to cells of the vascular cylinder between the xylem and phloem poles (Fig. 6*B*). The pattern was similar in plants grown at 0.1 and 10 $\mu$M iron (data not shown). Control *in situ* hybridization with *fer* sense probes revealed no signals (Fig. 6 *E* and *F*). Thus, the expression of *fer* occurred in a cell-specific pattern along the root irrespective of iron supply.

## Discussion

Our data comprising the *fer* mapping, the complementation studies with ORFb, and the DNA polymorphism in ORFb demonstrate that ORFb is the *fer* gene. Sequence comparisons revealed that *fer* encodes a bHLH protein. bHLH proteins are characterized by a conserved bHLH domain that has been demonstrated to be involved in DNA binding in eukaryotes (28). We therefore predict that the primary defect in the *fer* mutant is caused by a regulatory deficiency, presumably happening at transcriptional level through the interaction of FER with regulatory sequences of the FER target genes. We can exclude that the primary defect in *fer* is caused by a mutated metal transporter, iron reductase or $H^+$-ATPase.

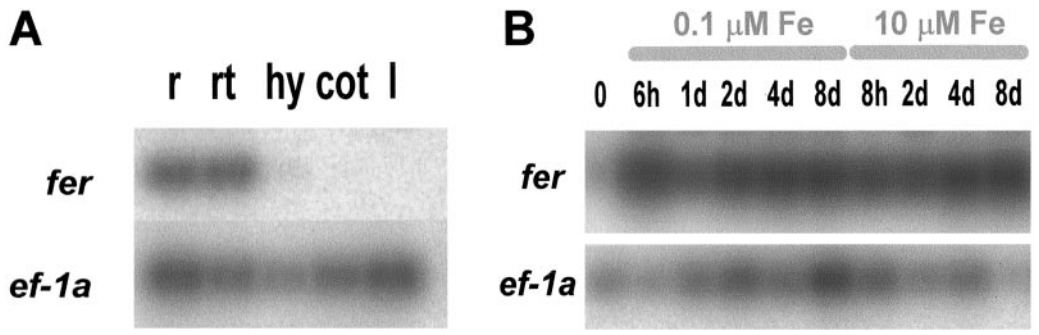


**Fig. 5.** RT-PCR expression analysis of the *fer* gene. (*A*) Expression in various tissues of tomato: r, entire roots; rt, root tips; hy, hypocotyls; cot, cotyledons; l, leaves. As positive control, expression of elongation factor *Leef-1a* was monitored. (*B*) Root expression in response to iron supply: 0, before the start of the experiment; 1d–8d, 1–8 days of growth after iron limitation (0.1 μM iron) or sufficient iron supply (10 μM iron).

We can demonstrate that in addition to the physiological alterations in response to iron limitation, *fer* mutant plants exhibit morphological phenotypes with respect to the root-hair growth and lateral root-elongation pattern at both low and sufficient iron supply. This shows that *fer* functions irrespective of the iron concentration in the medium. Consistent with the constant functioning of FER is the finding that *fer* is expressed in roots independently from iron-supply conditions. Presumably, the FER protein is present irrespective of the iron concentration such that the FER-mediated regulation of the iron responses does not likely happen at the *fer* transcriptional level. Thus, FER may act as a global regulator for iron uptake. As such FER should be able to respond to different iron concentrations to induce the appropriate responses in roots. To achieve this, FER may act together with other iron-signaling factors of yet unknown nature.

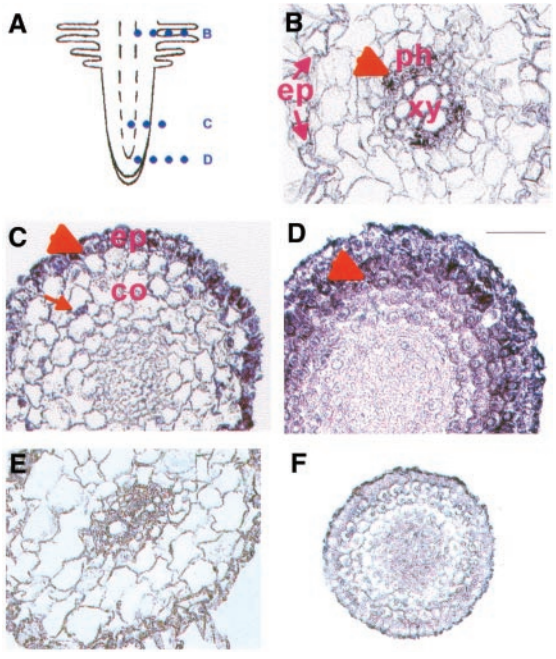


**Fig. 6.** Localization of *fer* expression by *in situ* hybridization. (*A*) Schematic representation of a longitudinal section through a root. Dotted lines indicate the locations of transverse sections analyzed in *B–D*. (*B–D*) *In situ* hybridization analysis of *fer* transcripts using a *fer* antisense probe on 10-μm transverse sections through root tips. The sections were derived from the mature root-hair zone (*B*), the elongation zone (*C*), and the dividing root zone after the meristem (*D*). ph, phloem; xy, xylem; ep, root epidermis; co, cortex. Red arrowheads indicate *fer* expression. The thin red arrow indicates weak *fer* expression in the cortex. (*E* and *F*) Control hybridization using a *fer* sense probe. No signal was detected.

The *fer*-grafting results (15) together with our *fer*-expression studies demonstrated that *fer* is active and required in roots only. Assuming that the cells that express *fer* are also the sites of FER action, we deduce that FER-mediated control of iron uptake takes place in the epidermal and to a minor degree in the outer cortical cell layers of the root tips. Root tips of lateral roots explore iron availability in the soil and thus would need to sense iron. Iron supply can influence lateral root elongation and initiation of root-hair formation near the tip. We predict that FER may be involved in iron sensing in the lateral root tip. For example, FER may be one of several regulators that can fuel into the root-hair developmental program, because root-hair formation is highly sensitive to a range of environmental factors (29, 30). Root-hair proliferation is not fully restored in the transgenic overexpressing *fer* plants. One possible explanation is that the cell-specific expression pattern of *fer* is important for root-hair proliferation, or that alternatively important regulatory sequences for the root-hair response were lacking in the otherwise complemented plants. With root differentiation, *fer* expression shifts to the vascular cylinder. The vascular cylinder is involved in long-distance transport. Presumably, iron is transported from the external root layers to the central cylinder, where it is translocated into the xylem and transported to the shoot in complexed form with carbonic acids (31). *fer* therefore may also be involved in regulating iron-transport processes in the vascular system. To date, the expression pattern we observed for *fer* has not been described for another iron-response gene yet. Rapid changes in expression patterns of iron-responsive genes are detected in the epidermis cells of the root-hair zone in *Arabidopsis* in response to iron supply (9, 32). Moreover, iron-reduction activity is seen in the epidermis of the root-hair zone in tomato (15). *Leirt1* expression depends on the *fer* gene. One possibility is that FER may bind directly to the promoters of the iron-reductase gene or *Leirt1*. Because *fer* is not expressed in the epidermis of the root-hair zone as might be expected from a regulator of these genes, an alternative possibility is that FER may not be a direct regulator for *irt1* and the reductase gene, but it may control another regulator, which then acts at the promoters of these iron-response genes.

The further characterization of the *fer* gene and its possible targets will permit a detailed investigation of the control of the iron-uptake mechanism of strategy I plants and the communication of plant roots with their environment. In addition, the isolation of *fer* may form the basis for the manipulation of plants to generate high-yielding, iron-efficient or iron-rich crops to contribute toward the improvement of iron deficiency in humans.

We thank K. Babuin, B. Knüpfer, D. Kriseleit, and C. Nussbaumer for technical assistance and E. Schlagenhauf for DNA sequence assembly. This work was supported by Deutsche Forschungsgemeinschaft Grants Ga470/2-2 (to M.G.) and Ba1610/2-3 (to P.B. and M.G.) and Swiss National Science Foundation Grant 31-55288.98 (to H.-Q.L. and B.K.).

1. Guerinot, M. L. (2000) *Science* **287,** 241–243.
2. World Health Organization (2002) *Battling Iron Deficiency Anaemia*, www.who.int/nut/ida.htm.
3. Wu, J., Boyle E., Sunda, W. & Wen, L.-S. (2001) *Science* **293,** 847–849.
4. Geider, R. J. (1999) *Nature* **400,** 815–816.
5. Guerinot, M. L. (2001) *Nat. Biotechnol.* **19,** 417–418.
6. Römheld, V. (1987) *Physiol. Plant.* **70,** 231–234.
7. Briat, J.-F. & Lobreaux, S. (1997) *Trends Pharmacol. Sci.* **2,** 187–193.
8. Schmidt, W. & Schikora, A. (2001) *Plant Physiol.* **125,** 2078–2084.
9. Vert, G., Grotz, N., Dedaldechamp, F., Gaymard, F., Guerinot, M. L., Briat, J. F. & Curie, C. (2002) *Plant Cell* **14,** 1223–1233.
10. Robinson, N. J., Procter, C. M., Connolly, E. L. & Guerinot, M. L. (1999) *Nature* **397,** 694–697.
11. Waters, B. M., Blevins, D. G. & Eide, D. J. (2002) *Plant Physiol.* **129,** 85–94.
12. Eide, D., Broderius, M., Fett, J. & Guerinot, M. L. (1996) *Proc. Natl. Acad. Sci. USA* **93,** 5624–5628.
13. Connolly, E. L., Fett, J. P. & Guerinot, M. L. (2002) *Plant Cell* **14,** 1347–1357.
14. Eckhardt, U., Mas Marques, A. & Buckhout, T. J. (2001) *Plant Mol. Biol.* **45,** 437–448.
15. Brown, J. C., Chaney, R. L. & Ambler, J. E. (1971) *Physiol. Plant.* **25,** 48–53.
16. Brown, J. C. & Ambler, J. E. (1974) *Physiol. Plant.* **31,** 221–224.
17. Ling, H.-Q., Pich, A., Scholz, G. & Ganal, M. W. (1996) *Mol. Gen. Genet.* **252,** 87–92.
18. Stephan, U. W. & Prochazka, Z. (1989) *Acta Bot. Neerl.* **38,** 147–153.
19. Martin, G. B., Ganal, M. W. & Tanksley, S. D. (1992) *Mol. Gen. Genet.* **233,** 25–32.
20. Stein, N., Feuillet, C., Wicker, T., Schlagenhauf, E. & Keller, B. (2000) *Proc. Natl. Acad. Sci. USA* **97,** 13436–13441.
21. Wicker, T., Stein, N., Alber, L., Feuillet, C., Schlagenhauf, E. & Keller, B. (2001) *Plant J.* **26,** 307–316.
22. Höfgen, R. & Willmitzer, L. (1990) *Plant Sci.* **66,** 221–230.
23. Ling, H.-Q., Kriseleit, D. & Ganal, M. W. (1998) *Plant Cell Rep.* **17,** 843–847.
24. Bauer, P., Crespi, M. D., Szecsi, J., Allison, L. A., Schultze, M., Ratet, P., Kondorosi, E. & Kondorosi, A. (1994) *Plant Physiol.* **105,** 585–592.
25. Pokalsky, A. R., Hiatt, W. R., Ridge, N., Rasmussen, R., Houck, C. M. & Shewmaker, C. K. (1989) *Nucleic Acids Res.* **17,** 4661–4673.
26. Kyozuka, J., Konishi, S., Nemoto, K., Izawa, T. & Shimamoto, K. (1998) *Proc. Natl. Acad. Sci. USA* **95,** 1979–1982.
27. Jackson, D. (1991) in *A Practical Approach in Molecular Plant Pathology*, eds, Bowles D. J., Gurr S. J. & McPherson M. (Oxford Univ. Press, Oxford), pp. 163–174.
28. Atchley, W. R. & Fitch, W. M. (1997) *Proc. Natl. Acad. Sci. USA* **94,** 5172–5176.
29. Schiefelbein, J. W. (2000) *Plant Physiol.* **124,** 1525–1531.
30. Forde, B. & Lorenzo, H. (2001) *Plant Soil* **232,** 51–68.
31. Lopez-Millan, A. F., Morales, F., Andaluz, S., Gogorcena, Y., Abadía, A., De Las Rivas, J. & Abadía, J. (2000) *Plant Physiol.* **124,** 885–898.
32. Vert, G., Briat, J.-F. & Curie, C. (2001) *Plant J.* **26,** 181–189.